Separation Science and Technology
Publication details, including instructions for authors and subscription information:
http://www.informaworld.com/smpp/title~content=t713708471

Modified Shrinking Core Model for Reversible Sorption on Ion-Exchange Resins

Vinay M. Bhandari[a]; Vinay A. Juvekar[a]; Suresh R. Patwardhan[a]
[a] DEPARTMENT OF CHEMICAL ENGINEERING, INDIAN INSTITUTE OF TECHNOLOGY, BOMBAY, INDIA

To cite this Article Bhandari, Vinay M. , Juvekar, Vinay A. and Patwardhan, Suresh R.(1992) 'Modified Shrinking Core Model for Reversible Sorption on Ion-Exchange Resins', Separation Science and Technology, 27: 8, 1043 — 1064
To link to this Article: DOI: 10.1080/01496399208019023
URL: http://dx.doi.org/10.1080/01496399208019023

SEPARATION SCIENCE AND TECHNOLOGY, **27**(8 & 9), pp. 1043–1064, 1992

Modified Shrinking Core Model for Reversible Sorption on Ion-Exchange Resins

VINAY M. BHANDARI, VINAY A. JUVEKAR,*
and SURESH R. PATWARDHAN

DEPARTMENT OF CHEMICAL ENGINEERING
INDIAN INSTITUTE OF TECHNOLOGY
BOMBAY 400076, INDIA

Abstract

A modified shrinking core model is proposed to correlate dynamics of acid sorption on weak base ion-exchange resins in free base form. The model considers reversibility of the sorption process which is ignored in the conventional shrinking core model. The model is easy to apply and is shown to yield results which are in agreement with a computationally intensive rigorous model. The model is successfully verified using the experimental data on sorption of strong acids (HCl and HNO_3) on weak base resins (Dowex WGR-2 and Amberlite IRA-93).

Key Words: Ion exchange; Acid sorption; Weak base resin; Shrinking core model; Modeling

INTRODUCTION

Sorption of mineral and organic acids from dilute aqueous solutions on fixed beds of weak base resins is a widely used process in water and industrial effluent treatments. Here the sorption occurs essentially under unsteady-state conditions. To design such a process it is necessary to incorporate a single particle dynamics sorption model into differential balance equations describing axial and temporal variations of concentration in the column. In order to ease the computational efforts associated with such simulations, it is necessary to have a single particle sorption dynamics model which is simple and yet sufficiently accurate. The shrinking core model, proposed by Helfferich in 1965 (*1*), has these attributes. A fair amount of work exists in the literature on the sorption of acids on weak base resins and application of the shrinking core model to ion-exchange dynamics (*1–8*). This model has also been applied to sorption studies on

*To whom correspondence should be addressed.

weak acid resins and chelate exchangers (*9–13*). The shrinking core model assumes a sharp boundary between the reacted shell of the resin particle and the unreacted core. The rate of sorption is assumed to be governed by the diffusion of the reactive species through the shell region under quasi-steady-state conditions. The major drawback of the shrinking core model in its application to the sorption of acids on weak base resins is that it is valid only in those cases where the reaction between the acid and the fixed ionogenic groups of the resin is irreversible. This assumption of irreversibility is not, in general, valid. Our previous studies (*14*, *15*) have shown that when sorption occurs from dilute acid solutions on resins which are relatively weak bases, a significant reversibility is observed in the sorption isotherm. The cause of this reversibility is shown to be a near total exclusion of H^+ ions from the double layer in the vicinity of the pore walls. Such situations cannot be modeled on the basis of the conventional shrinking core model. It should be noted that the situations where a dilute acid encounters a weak base resin are very common in practice, especially in water and process effluent treatments. Even in those cases where the feed solutions have relatively high concentrations of acids, there are regions in the vicinity of advancing concentration fronts (both inside resin particles and inside the resin bed) where the acid concentrations are low. Here the conventional shrinking core model may fail.

In the present study we have modified the conventional shrinking core model by incorporating the effect of reversibility of sorption. The modified shrinking core model retains the form of the conventional shrinking core model and is easily extendable to column dynamics. The model is verified by using the experimental data reported elsewhere (*14*) on the dynamics of sorption of strong acids (HCl and HNO_3) on weak base resins (Dowex WGR-2 and Amberlite IRA-93). Although the model developed here is applicable only to the sorption of strong acids, it can easily be extended to the sorption of weak acids by accounting for their incomplete dissociation.

DYNAMICS OF ACID SORPTION ON WEAK BASE RESINS

The first reaction step during the sorption of an acid, HA, on the free base form of a weak base resin is the protonation of fixed ionogenic groups of the resin by the H^+ ions from the solution:

$$\overline{R} + \overline{H} \rightleftarrows \overline{RH} \qquad (1)$$

Here $\overline{R}$ represents the fixed ionogenic species of the resin while $\overline{RH}$ represents its protonated form. $\overline{H}$ represents the H^+ ion. The bars above the species refer to an intraparticle environment. The protonation reaction is

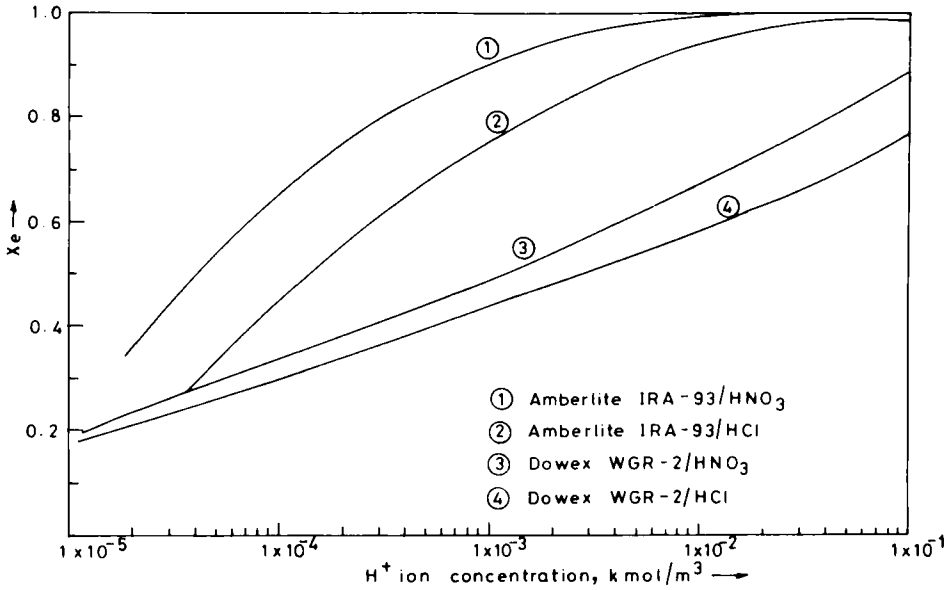

FIG. 1. Plot of X_e vs concentration.

instantaneous and, in general, reversible. Plots of equilibrium resin conversion, X_e (= $[\overline{RH}]/Q$, where $[\overline{RH}]$ is the concentration of the protonated species of the resin and Q is the resin capacity) vs [H] (H^+ ion concentration in the extraparticle solution) based on the experimental data of Bhandari et al. (*14*) are shown in Fig. 1. For an irreversible sorption, X_e should be equal to 1 over the entire range of H^+ ion concentration. Deviation from the rectangular isotherm, indicating a significant reversibility of the process, is amply demonstrated by Fig. 1. The cause of the reversibility of the protonation reaction is believed to be the exclusion of H^+ ions (coions) from the region adjacent to the solid–liquid interface. This coion exclusion is due to the formation of the electrical double layer in the vicinity of the positively charged pore walls. Bhandari et al. (*14*) proposed a reversible sorption model to describe both the sorption equilibria and sorption dynamics. This model is discussed here first, since it forms the basis of the modified shrinking core model.

In the reversible sorption model it is assumed that electroneutrality (i.e., $[\overline{H}] = [\overline{A}]$) exists at the axis of the pore or in a region surrounding the pore axis which is called the core region. As we move away from the pore axis toward the pore wall, disparity between the concentration of acid anion, A^-, and H^+ ions increases. The concentration of H^+ ions decreases

while the concentration of A^- ion increases from the pore axis to the pore wall. The product of the concentrations of H^+ and A^- ions is assumed to be a constant on the basis of the ideal form of the Donnan equilibrium, i.e.,

$$[\bar{H}]_s[\bar{A}]_s = [\bar{H}]_a[\bar{A}]_a = [H][A] \tag{2}$$

where the subscript s denotes the resin surface and the subscript a denotes the pore axis (or the core). [H] and [A] are the extraparticle concentrations.

The concentration of A^- ions in the vicinity of the pore wall is related to that in the core by the Freundlich-type equilibrium,

$$[\bar{A}]_s = [\overline{RH}]K\left(\frac{[\bar{H}]_a}{Q}\right)^n \tag{3}$$

Equilibrium constant, K_p, of the protonation reaction (Eq. 1) occurring at the pore wall is expressed as

$$K_p = \frac{[\overline{RH}]}{[\bar{R}][\bar{H}]_s} \tag{4}$$

Based on Eqs. (1), (2), and (3) and the balance on the active species of the resin,

$$Q = [\overline{RH}] + [\bar{R}] \tag{5}$$

the following equation is derived:

$$K_0 = \frac{K_p}{K} = \frac{[\overline{RH}]^2}{(Q - [\overline{RH}])[\bar{H}]_a^2}\left(\frac{[\bar{H}]_a}{Q}\right)^n \tag{6}$$

At equilibrium, the concentration of H^+ ions in the core region, $[\bar{H}]_a$, equals their concentration in the extraparticle solution. Hence the sorption isotherm relating the extraparticle concentration of H^+ ions and the concentration of the protonated form of resin can be written as

$$K_0 = \frac{[\overline{RH}]^2}{(Q - [\overline{RH}])[H]^2}\left(\frac{[H]}{Q}\right)^n \tag{7}$$

The concentration of H^+ ions at a distance ζ from the pore axis is related to their axial concentration by the following equation:

$$[\bar{H}]_\zeta = [\bar{H}]_a/\lambda(\zeta) \tag{8}$$

where $\lambda(\zeta)$ is the factor which accounts for the concentration variation in the pore and is, in general, a function of ζ, the distance from the pore axis.

Based on Eq. (8) and the ideal Donnan equilibrium, the following equation for the distribution of A^- ions in the pore may be written

$$[\overline{A}]_\zeta = [\overline{A}]_a \lambda(\zeta) \tag{9}$$

The dynamics of sorption is governed by diffusion of the ions in the pores. The flux of any ion i can be expressed in terms of its concentration C_i and electrical potential ϕ by using the Nernst–Planck equation.

$$J_i = -D_i\left(\nabla C_i + z_i C_i \frac{\mathcal{F}}{\mathcal{R}T}\nabla\phi\right) \tag{10}$$

Writing Nernst–Planck equations for H^+ and A^- ions at a point (ζ,r) and eliminating the $\nabla\phi$ term between them by using the no current condition, the following equation for the flux of the H^+ ions is obtained:

$$J_H(\zeta,r) = -D_H\left(\frac{D_A[\overline{A}]_\zeta(\partial[\overline{H}]_\zeta/\partial r) + D_A[\overline{H}]_\zeta(\partial[\overline{A}]_\zeta/\partial r)}{D_A[\overline{A}]_\zeta + D_H[\overline{H}]_\zeta}\right) \tag{11}$$

Here r is the location along the pore axis measured from the center of the resin particle. It is assumed that all the pores are straight and radially run from the center of the resin to the surface. The appropriate correction for the tortuosity of the pores is incorporated in the pore diffusivity terms. Equation (11) can be simplified by using Eqs. (8) and (9) to give

$$J_H(\zeta,r) = -\left(\frac{2D_A D_H}{\dfrac{D_H}{\lambda(\zeta)} + D_A\lambda(\zeta)}\right)\frac{\partial[\overline{H}]_a}{\partial r} \tag{12}$$

Based on Eq. (12), the area average flux at location r in a pore may be expressed as

$$\bar{J}_H = -D_{HA}\frac{\partial[\overline{H}]_a}{\partial r} \tag{13}$$

where D_{HA} is the effective pore diffusion coefficient which is given by

$$D_{HA} = \left(\frac{2D_A D_H}{\dfrac{D_H}{\bar{\lambda}} + \bar{\lambda}D_A}\right) \tag{14}$$

$\bar{\lambda}$ in Eq. (14) is an average value of $\lambda(\zeta)$ in the pore.

The unsteady-state material balance of H^+ ions in the pore may be written as

$$\frac{\partial[\overline{H}]_{av}}{\partial t} + \frac{\partial[\overline{RH}]}{\partial t} = -\frac{1}{r^2}\frac{\partial}{\partial r}(r^2\bar{J}_H) \tag{15}$$

$[\overline{H}]_{av}$ is the average concentration of $[\overline{H}]$ in the pore and may be approximately related to the core concentration $[\overline{H}]_a$ as

$$[\overline{H}]_{av} = [\overline{H}]_a/\bar{\lambda} \tag{16}$$

Equation (15) can be converted into that involving a single dependent variable $[\overline{H}]_a$ by using Eqs. (6), (13), and (16). The following boundary conditions are used in conjunction with the resulting equation:

$$\partial[\overline{H}]_a/\partial r = 0 \quad \text{at} \quad r = 0 \tag{17}$$

$$[\overline{H}]_a = [H] \quad \text{at} \quad r = R \tag{18}$$

and the initial condition to be used is

$$[\overline{H}]_a = 0 \quad \text{at} \quad t = 0 \tag{19}$$

When the concentration of acid in the extraparticle fluid [H] varies with time, the following equation may be written for the balance of H^+ ions in the extraparticle fluid:

$$\frac{d[H]}{dt} = \frac{3W[H]_i}{RQ}(\bar{J}_H|_{r=R}) \tag{20}$$

where W is a dimensionless resin loading which is defined as

$$W = \frac{4\pi R^3 N \epsilon_p Q}{3[H]_i} \tag{21}$$

N is the number of resin particles per unit volume of the extraparticle fluid, and ϵ_p is the fractional pore area of the resin. The initial condition for Eq. (20) is

$$[H] = [H]_i \quad \text{at} \quad t = 0 \tag{22}$$

TABLE 1
Characteristics of Resins

Resin	Dowex WGR-2	Amberlite IRA-93
Type	Epoxy amine polymer matrix	Polystyrene polyamine matrix
Capacity, kmol/m^3 (based on pore)	10.102	4.6709
Water content, m^3/kg dry resin	0.95	1.1775
Radius, m	2.45×10^{-4}	2.25×10^{-4}

The intraparticle dynamics equation (the modified form of Eq. 15) can be solved in conjunction with the extraparticle dynamics equation (Eq. 20) to simulate a batch dynamic process.

The above model was successfully validated using the experimental data on dynamics of sorption of HCl and HNO_3 from their aqueous solutions on Dowex WGR-2 and Amberlite IRA-93 resins (*14*). The characteristics of these resins are reported in Table 1, and the regressed values of D_{HA} obtained from the experimental data are given in Tables 2 to 5.

TABLE 2
Comparison of Values of Effective Diffusion Coefficient[a].
System: Amberlite IRA-93/HCl

$[HA]_i \times 10^3$ kmol/m^3	W	$D_{HA} \times 10^9$ m^2/s		
		SCM	RSM	MSCM
1.00	2.20	0.21	0.39	0.36
"	3.39	0.22	0.43	0.44
"	4.67	0.19	0.39	0.35
5.12	1.04	0.69	1.25	1.00
"	1.95	0.52	1.00	0.80
"	2.90	0.42	0.83	0.61
10.0	1.00	0.96	1.70	1.27
"	2.01	0.67	1.30	0.97
"	3.00	0.45	1.10	0.75
20.0	1.00	0.99	1.90	1.37
"	2.00	0.66	1.90	1.30

[a]SCM = shrinking core model. RSM = reversible sorption model. MSCM = modified shrinking core model.

TABLE 3
Comparison of Values of Effective Diffusion Coefficient[a].
System: Amberlite IRA-93/HNO_3

$[HA]_i \times 10^3$ kmol/m^3	W	$D_{HA} \times 10^9$ m^2/s		
		SCM	RSM	MSCM
1.00	2.34	0.33	0.55	0.47
"	4.22	0.20	0.46	0.31
"	5.79	0.23	0.40	0.33
4.50	0.93	0.92	1.20	1.06
"	1.30	0.67	0.95	0.78
"	1.70	0.55	0.94	0.67
9.77	0.80	1.19	1.75	1.46

[a]SCM = shrinking core model. RSM = reversible sorption model. MSCM = modified shrinking core model.

TABLE 4
Comparison of Values of Effective Diffusion Coefficient[a].
System: Dowex WGR-2/HCl

$[HA]_i \times 10^3$ kmol/m^3	W	$D_{HA} \times 10^9$ m^2/s		
		SCM	RSM	MSCM
1.12	2.50	0.98	3.00	2.57
"	3.00	0.74	2.85	2.37
"	4.00	0.74	2.85	2.54
5.11	1.43	0.72	2.35	2.04
"	2.12	0.61	2.35	2.10
"	3.05	0.56	2.35	1.92
9.50	1.11	0.44	1.10	0.86
"	2.00	0.40	1.15	1.02
20.0	1.00	0.38	0.90	0.66
"	1.50	0.40	1.00	0.74
"	2.00	0.43	1.20	1.09

[a]SCM = shrinking core model. RSM = reversible sorption model. MSCM = modified shrinking core model.

TABLE 5
Comparison of Values of Effective Diffusion Coefficient[a].
System: Dowex WGR-2/HNO_3

$[HA]_t \times 10^3$ kmol/m^3	W	$D_{HA} \times 10^9$ m^2/s		
		SCM	RSM	MSCM
1.00	2.57	1.08	3.10	3.23
"	3.71	1.01	3.50	3.03
"	5.70	0.98	3.60	3.35
4.50	1.01	0.79	2.45	1.92
"	2.20	0.65	2.00	1.57
"	3.02	0.65	2.00	1.70
9.80	1.04	0.64	1.50	1.24
"	2.00	0.58	1.50	1.36

[a]SCM = shrinking core model. RSM = reversible sorption model. MSCM = modified shrinking core model.

THE MODIFIED SHRINKING CORE MODEL

Figure 2 shows simulated concentration profiles of the reacted form of the resin (i.e., $[\overline{RH}]$) at various instants of time during a run. These simulations are based on the reversible sorption model discussed in the previous section. The following observations are made from this figure. First, $[\overline{RH}]$, the concentration of the protonated form of resin, is less than the resin capacity Q at all the points in the reacted shell of the resin. Thus the reacted shell is not completely consumed. Second, the boundary between the shell and the unreacted core is not sharp. Both these phenomena are the results of reversibility of the sorption process. In the following text we have attempted to approximate this profile by using a core–shell type distinction.

Figure 3 shows a typical plot of fractional local conversion of resin X ($= [\overline{RH}]/Q$) vs dimensional radial location y ($= r/R$). Here X_e represents the value of X at the outer surface of the resin. It should be noted that every point on the resin surface is in equilibrium with the extraparticle solution. Hence X_e for any particular value of [H] can be obtained from Fig. 1. It can also be calculated using Eq. (23) which is obtained by rearrangement of Eq. (7):

$$X_e = \frac{-K_0[H]^2 + \sqrt{(K_0[H]^2)^2 + 4K_0Q^{1-n}[H]^{n+2}}}{2Q^{1-n}[H]^n} \tag{23}$$

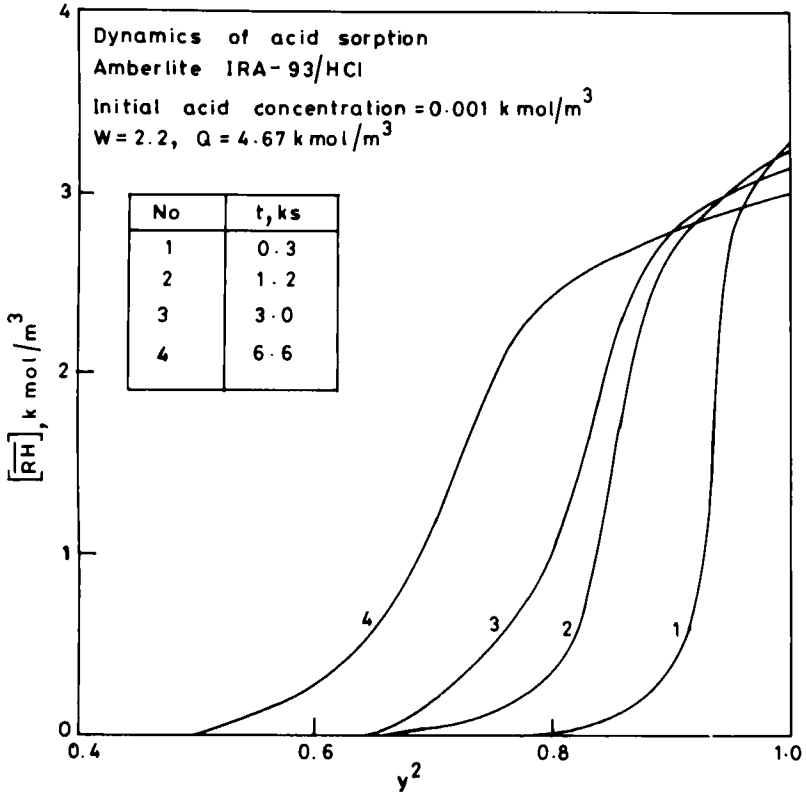

FIG. 2. Concentration profile inside resin particle.

The total quantity of the acid sorbed on a resin particle can be obtained from this plot by the following equation:

$$S_T = \int_0^R \epsilon_p[\overline{RH}]4\pi r^2 dr \tag{24}$$

$$= \epsilon_p Q 4\pi R^3 \int_0^1 Xy^2 dy \tag{25}$$

The global conversion, $\overline{X}$, of the resin can be obtained from S_T by using the following equation:

$$\overline{X} = \frac{S_T}{\frac{4}{3}\pi R^3 Q \epsilon_p} = 3\int_0^1 Xy^2 dy \tag{26}$$

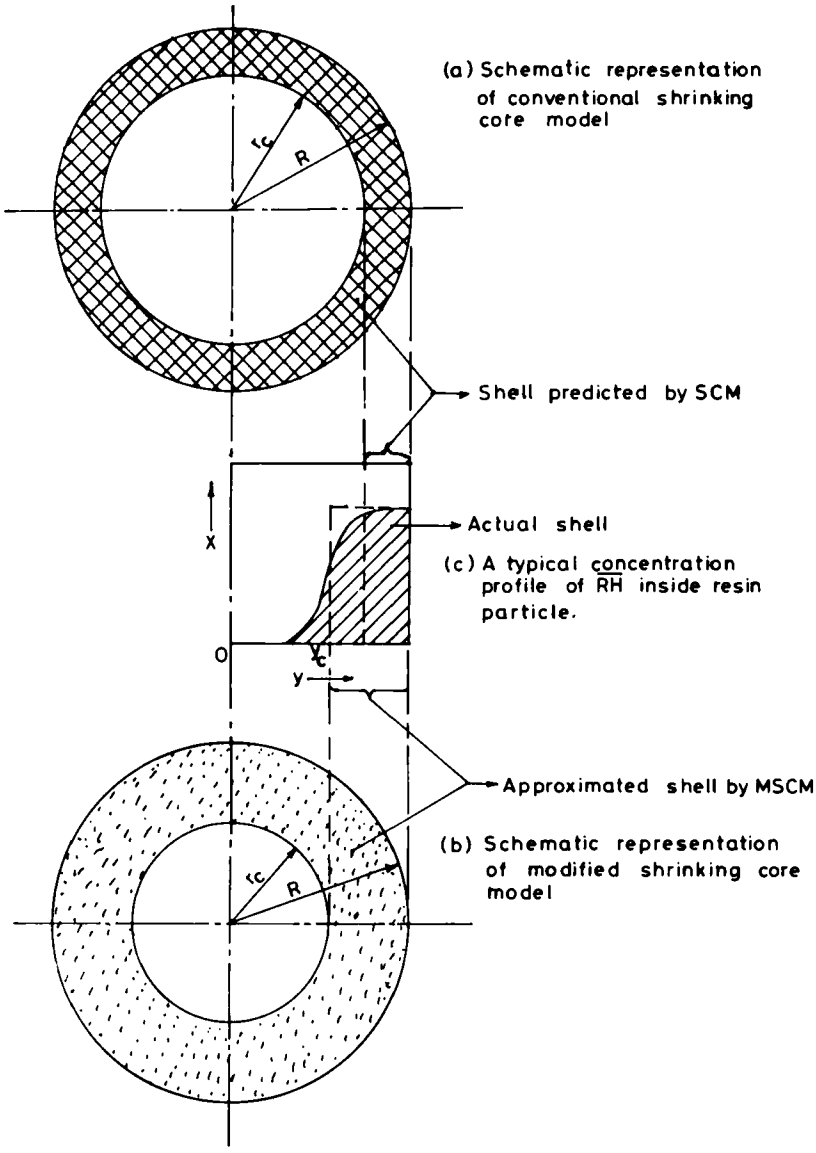

FIG. 3. Schematic representation of core–shell boundary.

As an approximation, we now replace the actual profile of X with a rectangular profile with height X_e and extending up to the dimensionless radius y_c ($= r_c/R$). Here r_c represents the fictitious core radius that should be adjusted in such a way that the total acid sorbed by the resin particle is now contained in the uniformly dense shell (with conversion X_e) extending from r_c to R. Hence we can write

$$\frac{4}{3}\pi(R^3 - r_c^3)X_e = \frac{4}{3}\pi R^3 X \tag{27}$$

or

$$y_c = \frac{r_c}{R} = \left[1 - \frac{\overline{X}}{X_e}\right]^{1/3} \tag{28}$$

We now extend the treatment of the conventional shrinking core model to this modified shell–core picture of the resin.

Quasi-steady-state equation for the diffusion of H^+ ions in the shell region may be written as

$$\frac{1}{r^2}\frac{\partial}{\partial r}(\bar{J}_H) = 0 \tag{29}$$

Substituting $\bar{J}_H$ from Eq. (13) into Eq. (29), we get

$$D_{HA}\frac{1}{r^2}\frac{\partial}{\partial r}\left(r^2\frac{\partial[\overline{H}]_a}{\partial r}\right) = 0 \tag{30}$$

Boundary conditions to be used in conjunction with Eq. (30) are

$$[\overline{H}]_a = 0 \quad \text{at} \quad r = r_c \tag{31}$$

$$[\overline{H}]_a = [H] \quad \text{at} \quad r = R \tag{32}$$

Integrating Eq. (30) twice and using the boundary conditions to evaluate the constants of integration, we get the following expression for the concentration profile of H^+ ion:

$$[\overline{H}]_a = [H]\frac{\left(\frac{1}{r_c} - \frac{1}{r}\right)}{\left(\frac{1}{r_c} - \frac{1}{R}\right)} \tag{33}$$

The flux of H^+ ions at the core–shell boundary ($\bar{J}_H|_{r=r_c}$) can be obtained from Eqs. (13) and (33) as

$$\bar{J}_H|_{r=r_c} = -D_{HA}\frac{\partial[\overline{H}]_a}{\partial r}\bigg|_{r=r_c} = -\frac{D_{HA}[H]}{r_c^2\left(\frac{1}{r_c}-\frac{1}{R}\right)} \tag{34}$$

Material balance of H^+ ions at $r = r_c$ yields

$$\epsilon_p 4\pi r_c^2 Q X_e \frac{dr_c}{dt} = \epsilon_p 4\pi r_c^2 \bar{J}_H|_{r=r_c} \tag{35}$$

It should be noted that in writing the above material balance we have used the utilized capacity of the reacted shell, QX_e, rather than the total capacity Q used in the conventional shrinking core model.

Substituting $\bar{J}_H|_{r=r_c}$ from Eq. (34) in Eq. (35) and further simplifying, we get

$$\frac{dr_c}{dt} = -\frac{D_{HA}}{QX_e}\frac{[H]}{r_c^2\left(\frac{1}{r_c}-\frac{1}{R}\right)} \tag{36}$$

Equation (36) is subjected to the following initial condition:

$$r_c = R \quad \text{at} \quad t = 0 \tag{37}$$

Solution of Eq. (36) yields the following expression:

$$\frac{6D_{HA}}{QX_eR^2}\int_0^t [H]dt = \left[1 - 3\left(\frac{r_c}{R}\right)^2 + 2\left(\frac{r_c}{R}\right)^3\right] \tag{38}$$

Substituting the expression for r_c/R from Eq. (28) into Eq. (38), we get the final equation for the modified shrinking core model:

$$\frac{6D_{HA}}{QR^2X_e}\int_0^t [H]dt = \left[1 - 3\left(1 - \frac{\overline{X}}{X_e}\right)^{2/3} + 2\left(1 - \frac{\overline{X}}{X_e}\right)\right] \tag{39}$$

It should be noted that both $\overline{X}$ and X_e are functions of time.

Equation (39) predicts that the plot of $X_e[1 - 3(1 - (\overline{X}/X_e))^{2/3} + 2(1 - (\overline{X}/X_e))]$ vs $\int_0^t [H]dt$ is a straight line passing through the origin and having the slope $6D_{HA}/QR^2$.

The conventional shrinking core model assumes complete utilization of the resin capacity ($X_e = 1$). The modified shrinking core model equation can readiy be converted to the conventional form by substituting $X_e = 1$ in Eq. (39), i.e.,

$$\frac{6D_{HA}}{QR^2}\int_0^t [H]dt = [1 - 3(1 - \overline{X})^{2/3} + 2(1 - \overline{X})] \qquad (40)$$

RESULTS AND DISCUSSION

To validate the modified shrinking core model using the experimental data on the sorption of HCl and HNO_3, the following procedure is used. The values of X_e for various values of [H] are obtained from Fig. 1. The value of global conversion $\overline{X}$ at time t is obtained from measurements of the total quantity of the acid sorbed between times 0 and t.

Figures 4 to 7 show plots of $WX_e[1 - 3(1 - (\overline{X}/X_e))^{2/3} + 2(1 - (\overline{X}/X_e))]$ (denoted by F in these figures) vs $W\int_0^t [H]dt$ for a few experimental runs. W is used here as a scale factor both in the abcissa and the ordinate. It is clear from these plots that Eq. (39) holds over practically

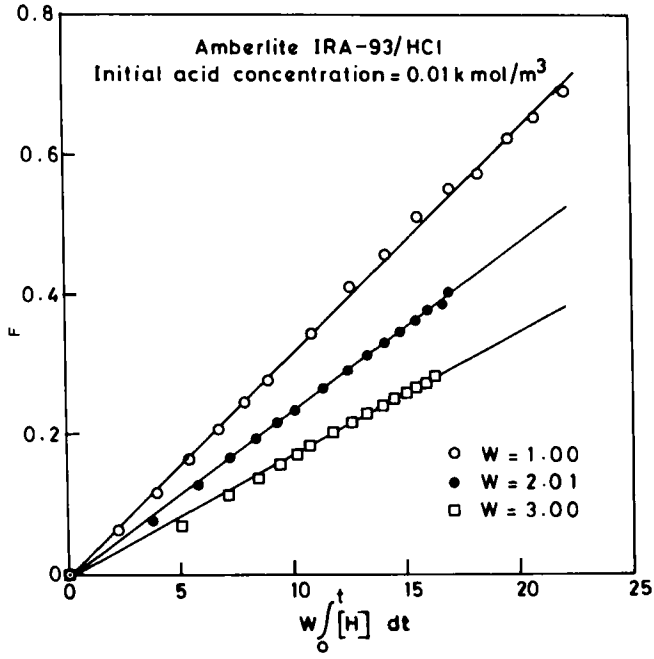

FIG. 4. Correlation of the experimental data using the modified shrinking core model.

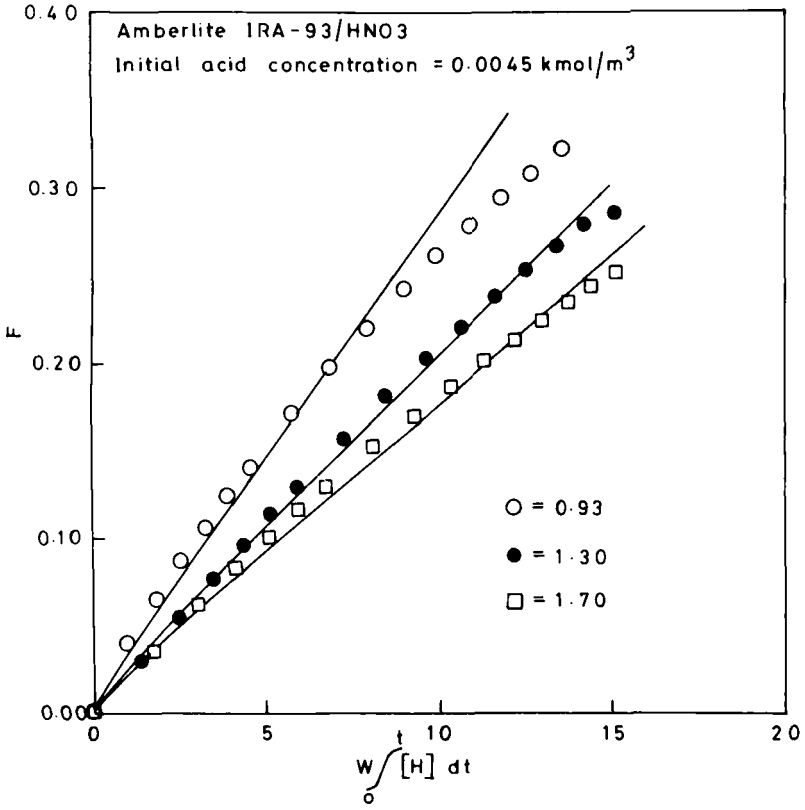

FIG. 5. Correlation of the experimental data using the modified shrinking core model.

the entire span of the acid concentration covered during an experiment. Deviations are observed at the points where $\overline{X}$ is very close to X_e. This is due to the fact that F is highly sensitive to the experimental errors in this region of the plots because of the terms in F which contain $(1 - \overline{X}/X_e)$. Tables 2 to 5 compare the values of the effective diffusion coefficient, D_{HA}, obtained from the slopes of these plots with those obtained by using the reversible sorption model described in an earlier section. Agreement between these values is fair (average deviation = 17% and maximum deviation = 32%), indicating the validity of the modified shrinking core model.

In many previous studies it was tacitly assumed that the reaction is irreversible, and the conventional shrinking core model was used for correlating the particle dynamics data. It is instructive to fit the conventional shrinking core model (Eq. 40) to the experimental data. This is attempted

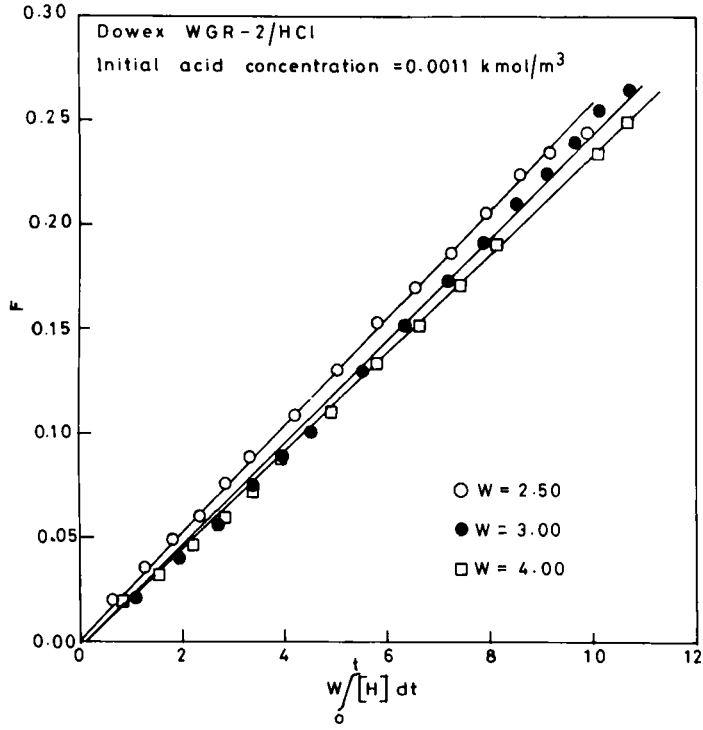

FIG. 6. Correlation of the experimental data using the modified shrinking core model.

in Figs. 8 to 11. In order to facilitate direct comparison between the modified and conventional shrinking core model, the experimental data used in these figures correspond to those used in Figs. 4 to 7, respectively. It is seen from these plots that although the conventional shrinking core model deviates significantly from the experimental data in the later portion of the dynamics, it does fit over a significant initial portion of the data. If only the initial portion of the data is available, it may mislead one to believe that the conventional shrinking core model is applicable to the sorption dynamics. However, the values of effective diffusivity obtained from the slopes of the straight-line portions of the plots in Figs. 8 to 11 are much lower than the corresponding values obtained from Figs. 4 to 7 (which are based on the modified shrinking core model). The lower values of the effective pore diffusion coefficient, D_{HA}, obtained from the conventional shrinking core model may be explained as follows. The conventional model assumes total filling of the shell ($X_e = 1$) as compared to the partial filling assumed by the modified shrinking core model. Thus, for the same quantity

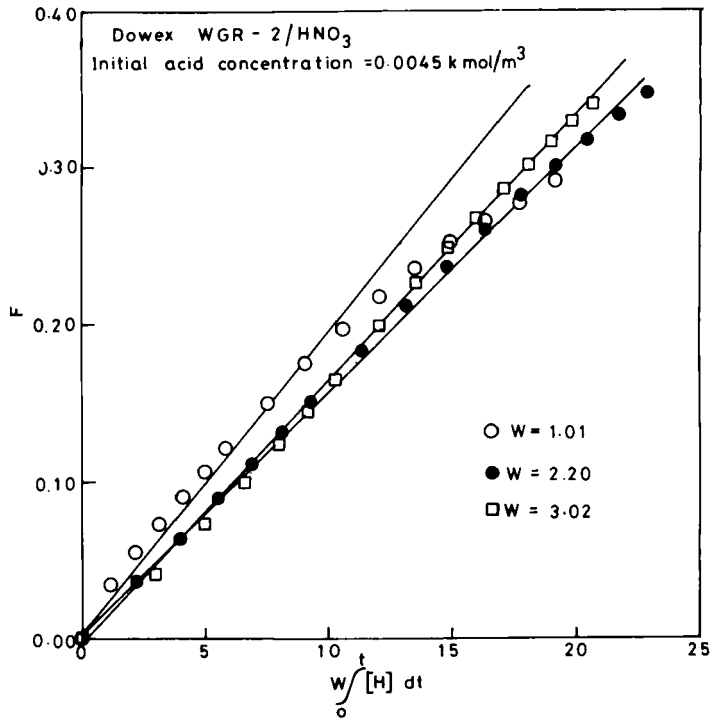

FIG. 7. Correlation of the experimental data using the modified shrinking core model.

of sorbed acid, the conventional model predicts a thinner shell and hence a shorter diffusion path than the modified shrinking core model (this is schematically shown in Fig. 3). Due to the shorter diffusion path, a smaller value of the diffusivity is sufficient in the conventional model to yield the same rate of sorption. Thus the conventional shrinking core model, although it appears to fit the data over a certain portion of dynamics, yields incorrect values of the effective pore diffusion coefficient. Tables 2 to 5 also list the values of D_{HA} obtained by using the conventional shrinking core model for all the runs. Comparison of these values with those of the reversible sorption model shows that the conventional model has an average deviation of 56.5% and a maximum deviation of 76%.

CONCLUSIONS

It is clear that the conventional shrinking core model has limited validity and should be used with caution. On the other hand, the modified shrinking core model, which combines the concept of reversibility with the shrinking

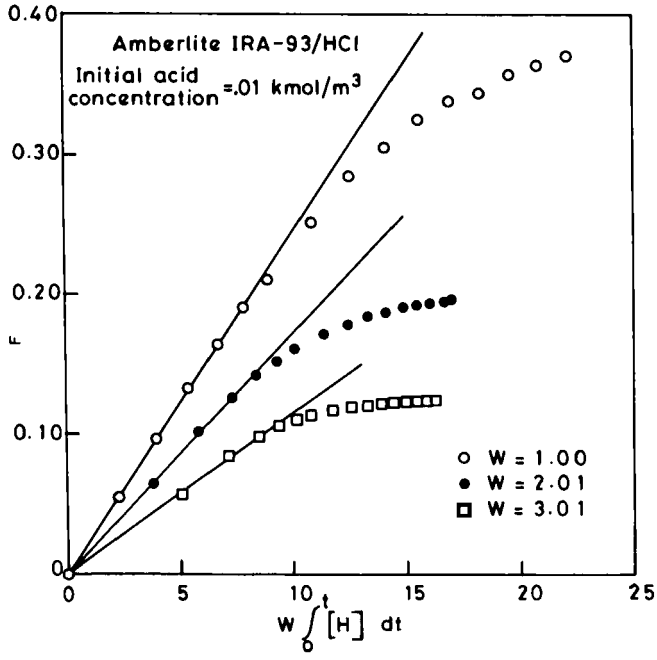

FIG. 8. Correlation of the experimental data using the conventional shrinking core model.

core model, is reliable. Although this model is somewhat less accurate than the rigorous model, it considerably simplifies the design procedure of the ion-exchange process and is particularly useful for obtaining quick estimates of exchange rates without much loss of accuracy.

NOMENCLATURE

A^-	anion species of the acid
C	concentration (kmol/m^3)
D_{HA}	effective pore diffusivity (m^2/s)
D_A	pore diffusivity of anion (m^2/s)
D_H	pore diffusivity of H^+ ion (m^2/s)
D_i	pore diffusivity of species i (m^2/s)
HA	acid species
[A]	concentration of acid anion (kmol/m^3)
[H]	concentration of H^+ ion (kmol/m^3)
[HA]	concentration of acid in solution (kmol/m^3)
K	adsorption equilibrium constant
K_0	equilibrium constant as defined in Eq. (6)

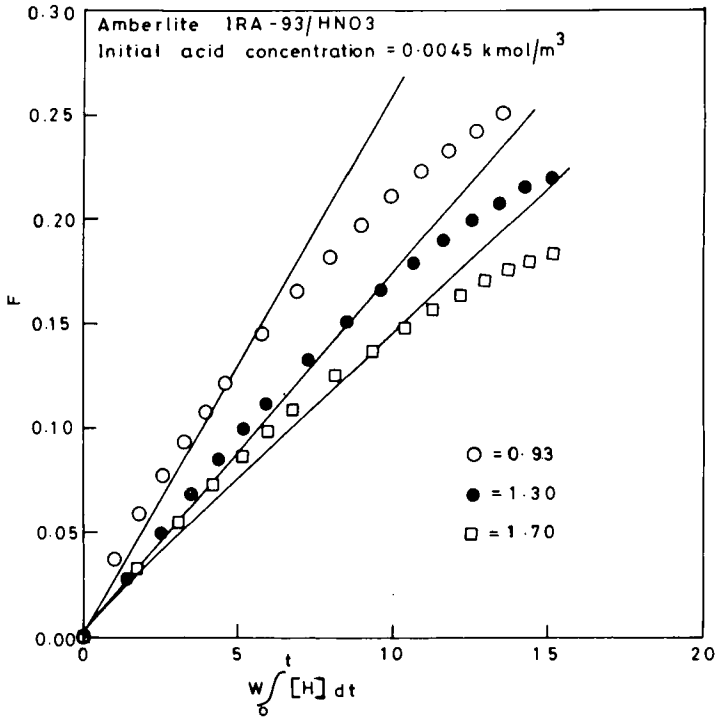

FIG. 9. Correlation of the experimental data using the conventional shrinking core model.

K_p	protonation equilibrium constant $(\text{kmol/m}^3)^{-1}$
N	number of resin particles per unit volume of extraparticle fluid
n	equilibrium constant as defined by Eq. (3)
Q	resin capacity based on pore volume (kmol/m^3)
R	radius of resin bead (m)
$\overline{\text{R}}$	free base group of resin
$\overline{\text{RH}}$	sorbed species of resin
r	radial distance measured from the center of bead (m)
r_c	unreacted core radius (m)
$[\overline{\text{R}}]$	concentration of free base group (kmol/m^3)
$[\overline{\text{RH}}]$	concentration of sorbed species (kmol/m^3)
S_T	quantity of acid sorbed (kmol)
t	time (s)
W	dimensionless resin loading
X	fractional conversion of the resin
$\overline{X}$	global fractional conversion of the resin

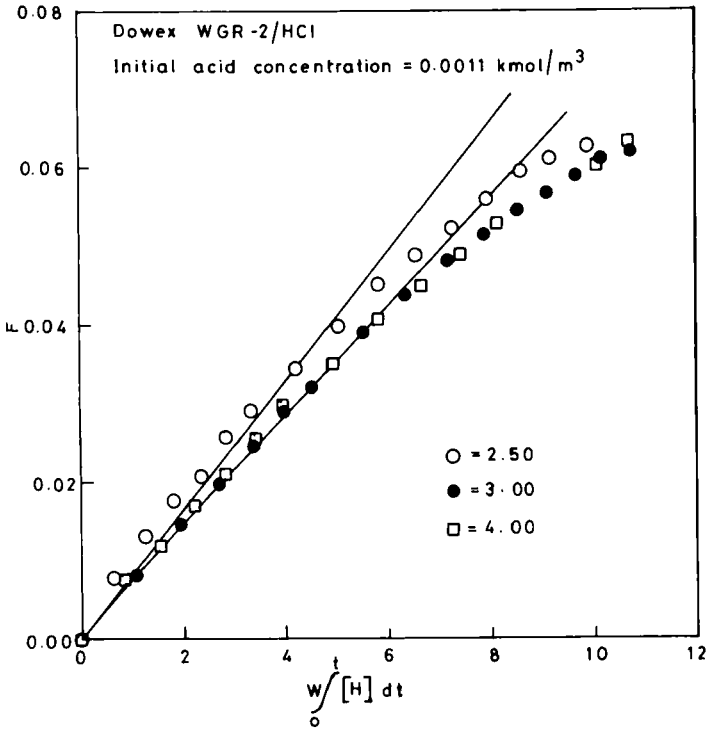

FIG. 10. Correlation of the experimental data using the conventional shrinking core model.

X_e fractional conversion of the resin at equilibrium
y (r/R)
Bar indicates resin phase

Subscript

a region surrounding pore axis
s surface
av average
i initial

Greek

ϕ electrical potential
ζ distance from the pore axis
λ factor as defined by Eq. (8)
$\bar{\lambda}$ average value of λ
ϵ_p fractional pore volume

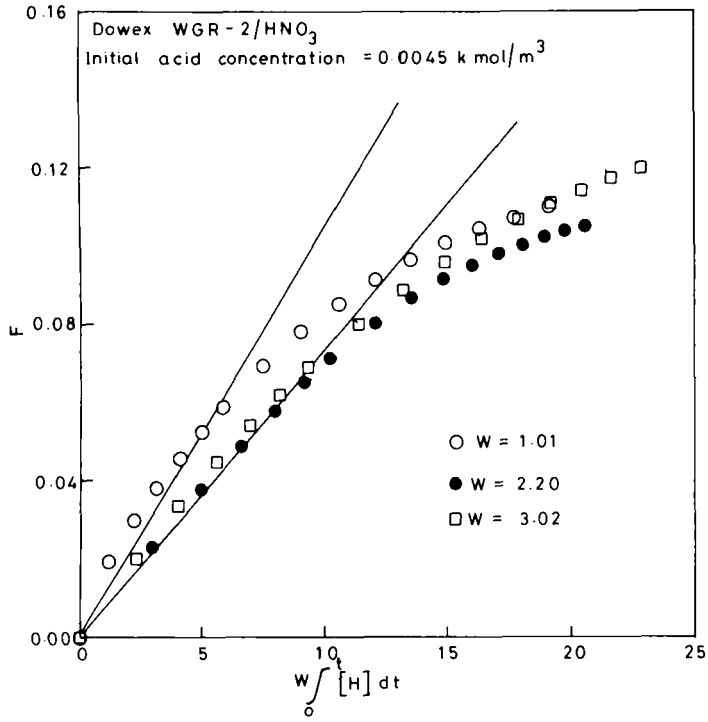

FIG. 11. Correlation of the experimental data using the conventional shrinking core model.

REFERENCES

1. F. Helfferich, "Ion-Exchange Kinetics (V). Ion Exchange Accompanied by Reactions," *J. Phys. Chem.*, *69*, 1178 (1965).
2. R. Kunin, *Ion-Exchange Resins*, Wiley, London, 1958.
3. F. Helfferich, *Ion Exchange*, McGraw-Hill, New York, 1962.
4. G. Adams, P. M. Jones, and J. R. Miller, "Kinetics of Acid Uptake by Weak Base Anion Exchangers," *J. Chem. Soc., Sec. A*, p. 2543 (1969).
5. P. Hubner and V. Kadlec, "Kinetic Behavior of Weak Base Anion Exchangers," *AIChE J.*, *24*, 149 (1978).
6. M. G. Rao and A. K. Gupta, "Ion Exchange Processes Accompanied by Ionic Reactions," *Chem. Eng. J.*, *24*, 181 (1982).
7. M. G. Rao and A. K. Gupta, "Kinetics of Ion Exchange in Weak Base Anion Exchange Resins," *AIChE Symp. Ser.*, *219*(78), 96 (1982).
8. F. G. Helfferich and Y. L. Hwang, "Kinetics of Acid Uptake by Weak Base Anion Exchangers. Mechanism of Proton Transfer," *Ibid.*, *242*(81), 17 (1985).
9. M. Nativ, S. Goldstein, and G. Schmukler, "Kinetics of Ion Exchange Processes Accompanied by Chemical Reactions," *J. Inorg. Nucl. Chem.*, *37*, 1951 (1975).
10. W. Höll and H. Sontheimer, "Ion Exchange Kinteics of the Protonation of Weak Acid Ion Exchange Resins," *Chem. Eng. Sci.*, *32*, 755 (1977).

11. W. Höll, "Optical Verification of Ion Exchange Mechanism in Weak Electrolyte Resins," *Reactive Polym., 2,* 93 (1984).
12. T. Kataoka and H. Yoshida, "Intraparticle Mass Transfer in Weak Acid Exchanger," *Can. J. Chem. Eng., 59,* 475 (1981).
13. H. Yoshida, T. Kataoka, and S. Fujikawa, "Kinetics in a Chelate Ion Exchanger (I). Theoretical Analysis," *Chem. Eng. Sci., 41,* 2517 (1986).
14. V. M. Bhandari, V. A. Juvekar, and S. R. Patwardhan, "Sorption Studies on Ion Exchange Resins. I. Sorption of Strong Acids on Weak Base Resins." Ind. Eng. Chem. Res., in press (1992).
15. V. M. Bhandari, V. A. Juvekar, and S. R. Patwardhan, "Sorption Studies on Ion Exchange Resins. II. Sorption of Weak Acids on Weak Base Resins." Ind. Eng. Chem. Res., in press (1992).

Received by editor August 12, 1991